Morphological analysis of bitumen phases using Atomic Force Microscopy

José P Aguiar-Moya, Ph.D., Jorge Salazar-Delgado, Vivian Bonilla-Mora, Ellen Rodríguez-Castro, Fabricio Leiva-Villacorta, Ph.D., Luis Loría-Salazar, Ph.D.

National Laboratory of Materials and Structural Models (LanammeUCR)
University of Costa Rica, P.O.Box 11501-2060, UCR, San José, Costa Rica

jose.aguiar@ucr.ac.cr

ABSTRACT.

The structure of asphalt is generally considered to be a colloidal system where high molecular weight components (asphaltenes) are dissolved into an oily lower molecular weight matrix (maltenes). To better understand the morphology of the asphalt binder, the different components associated with this material were analyzed under topographic and phase detection atomic force microscopy (AFM), and optical microscopy, for a specific asphalt binder type. The analyzed asphalt binder was identified as a multi-phase type asphalt binder that exhibits four distinct phases: the para-phase which serves as a dispersing medium to the catana-phase ("bee" structure), the per-phase (area surrounding the catana-phase), as well as the sal-phase (smaller dispersed phase). A component analysis of the asphalt binder yielded that a form of the per-phase and catana-phase can be associated to the aromatics. The sal-phase was observed on the asphaltenes and resins. Furthermore, an additional filament-type structure was also identified on the resins.

The analysis was also complemented by combining individual SARA components of the asphalt binder to observe the evolution of the different structures and morphology present in the asphalt binder. Furthermore, enriched asphalt binder with 50% of each of the SARA fraction at a time was also analyzed. It was determined that the size and shape of the different structures is a function of the combination of the different asphalt components. The effect of polymer modification and aging due to temperature were briefly analyzed. The results were also correlated to detailed infrared spectroscopy (FTIR) analysis of the different asphalt components.

KEYWORDS: AFM, FTIR, Asphaltenes, Saturates, Resins, Aromatics

1.0 Introduction

Modeling of asphalt bitumen is usually performed under the assumption that the material behaves as a Newtonian fluid, where viscosity is independent of shear strain rate, or as a non-Newtonian fluid (shear thinning), where viscosity does depend on the shear strain rate (Krishnan & Rajagopal, 2005). The former is typically associated with neat bitumens, while the latter is generally associated to polymer modified bitumens (West et al., 2010). At the molecular level, the shear thinning phenomena can be explained by entanglement of the polymer chains (Macoski, 1993). Consequently, the performance of the bitumen, and how it changes with time due to aging, oxidation, healing, and other processes associated with the material is a function of its chemical composition.

It has been clearly established in literature that the asphalt bitumen is a heterogeneous material, with large variations in constituents and composition (Jäger et al, 2004). The composition is more complex when modifiers are also considered. In general, the asphalt bitumen is a mixture of hydrocarbons that can become complex in nature (AI, 1989). Therefore, the heterogeneity of the material can be explained at the molecular-, nano-, and micro-scales. Furthermore, previous research has also demonstrated the presence of considerable spatial variability within these different length scales (Masson et al., 2006).

Then, because the macroscopic behaviour of the asphalt bitumen is directly influenced by the properties of the material at the smaller length scales, nano-scale material analysis, thermodynamic analysis, and chemical analysis are currently being employed to better understand the material. These approaches can also be used to design and engineer asphalts with properties that better adapt to the requirements of different projects in terms of stiffness, visco-elasticity and plasticity, adhesion and resistance to moisture, and resistance to fracture (Allen et al., 2012).

The following paper evaluates the composition and distribution of the various components of the asphalt bitumen (saturates, asphaltenes, resins, and aromatics) by themselves, as well as "enriched" asphalt bitumen with the different components (asphalt bitumen with an increased SARA fractions content), by means of atomic force microscopy (AFM). The roughness and different phases and structures within each component are also analyzed. This allows for a description of the different components and identification of the source of structures such as the so called "bee" structures within the asphalt bitumen matrix. The AFM analysis of the four bitumen components is also related to the measured Fourier-transformed infrared spectrums (FTIR). Finally, the effect on asphalt bitumen morphology due to polymer modification and heating is briefly analyzed.

2.0 Background

To date, there is an increasing interest in understanding the micro-mechanical and chemical behavior of bitumen to better model the performance of asphalt mixtures during their service life (Allen, 2010). Even though asphalt bitumen corresponds to a small percentage of the overall asphalt volume, variations in the molecular distribution and micro-mechanical arrangement of the different components in the bitumen, have a considerable impact in the performance of the asphalt mixture. The previous is due to the fact that small variations in the chemical and structural composition of the asphalt bitumen matrix have an effect on the rheological and thermoplastic behavior of the material (Allen, 2010).

However, proper characterization of the chemical and the micro-mechanical arrangement of the bitumen is difficult because even within a given bitumen source, considerable variation has been reported. When different sources are considered, the variation of the bitumen components has been described as high (Masson et al., 2006). Furthermore, several different phases, ranging from 4 to 6, have been identified within different asphalt binder sources (Jäger et al., 2004; Masson et al., 2006; Masson et al., 2007).

Consequently, various techniques have been used to characterize the chemical composition of the asphalt bitumen: Fourier transformed infrared spectroscopy (FTIR), Raman spectroscopy, X ray diffraction, electron microscopy, gas chromatography coupled to mass spectrometry, visible UV spectrometry, high-performance liquid chromatography (HPLC), Iatroscan or column chromatography, and Inductively coupled plasma mass spectrometry (ICP-MS). Similarly, techniques such as the following can be used to analyze the nano- and micro-mechanical structure and behavior of the asphalt bitumen: dynamic shear rheometer (DSR), dynamic mechanical analyzer (DMA), and atomic force microscopy. The previous techniques can also be used with thermal analysis to better understand the behavior of the material.

3.0 AFM Technique and Capabilities

A nanotechnology technique that has recently gained increased attention for characterizing the behavior of asphalt bitumen is the atomic force microscopy (AFM) (Nazzal & Qtaish, 2012). The technique was developed to overcome the limitations associated with scanning tunneling microscopy which requires that the material surface to be analyzed be a semiconductor. Consequently, in 1996, Binnig, Quate, and Gerber developed the atomic force microscope (Burnham & Colton, 1989).

The AFM has been designed to measure the forces that are generated between a tip that is attached to a cantilever beam and the material that is being evaluated, as a function of the separation between these two structures. Current AFM systems use a

laser beam deflection system that was initially developed by Meyer and Amer in 1988 (Meyer & Amer, 1988; Beaulieu, 2006). The laser is reflected from the back of the reflective AFM cantilever into a position-sensitive detector (PSD) that consists of two photodiodes. Consequently, displacement of the cantilever results in a difference in the signal collected between the two, which can be translated to proportional deflections of the cantilever. The system allows for a three-dimensional surface profile of a given sample.

The AFM can work in several modes: contact mode (CM), tapping mode or dynamic-force mode (DFM), and non-contact (AC) mode. Because of the composition and topography of asphalt bitumen, non-contact mode is generally preferred since it minimizes the normal and lateral forces (adequate for soft or viscous materials). Under AC mode, the forces between the sample and the tip are quite small and consequently the measurements are based on the resonant frequency or amplitude of the cantilever. Furthermore, depending on the capabilities of the system, lateral force microscopy (allows for measure of friction), force modulation (mechanical properties of the material, eg. Modulus of elasticity), and phase imaging (differences in properties of the asphalt binder: eg. adhesion, viscosity) can be assessed (Roa et al., 2011).

3.1 Characterization of Asphalt Bitumen with AFM

One of the initial AFM studies involving asphalt bitumen was performed by Loeber et al. (1996). The researchers obtained low resolution images that showed asphaltene molecules within a bitumen gel or matrix. Additionally, the authors observed randomly distributed "bee-shaped" structures within the asphalt bitumen matrix.

Jäger et al. (2004), indicated that the morphology of the bitumen was divided into the area corresponding to the "bee" structure (alternating high and low components), and two sub domains surrounding it (difference in topography of 5 μm). The authors indicated that the areas with higher stiffness exhibit less adhesive behavior. The "bee" structures were identified as string-like structures that emerge and immerse in the binder surface.

Masson et al. (2006), analyzed 13 asphalt bitumens by means of phase imaging AFM. The research allowed for the observation of several previously unseen morphologies and the classification of asphalt bitumen within 3 different groups: 1) fine dispersion (0.1-0.7 μm) in homogeneous matrix, 2) domains of 0.1 μm, and 3) 4 different phases of different sizes (catana-, per-, para-, and sal-phases). However, no correlation was identified between the AFM morphology and the four components in asphalt bitumen (saturates, asphaltenes, resins, and aromatics). No proof that the bitumen corresponds to a colloidal system (asphaltenes are stabilized by resins, and float in aromatics and saturates) was obtained.

Allen et al. (2012), found that prior to aging, asphalt bitumen showed two distinct phases: a continuous and a dispersed phase. The size of the dispersed phase is variable but ranges from 1-6 μm. The authors also identified that long-term aging results in micro-structural changes in the bitumen structure: phase dispersion, clustering, and materialization. The authors found that the "bee" structures are the results of the latter process, where a new sub-phase is identified within the dispersed phase. Aging also resulted in changes to the properties of each of the phases: stiffness.

McCarron et al. (2012), suggests that the "bee" structures are related to the waxy components in the asphalt bitumen (eg. long alkyl chain asphaltenes). The authors based the assumption on previous research by Moraes et al. (2010), who hypothesized that the "bee" structures are the result of crystallized wax within the bitumen. McCarron et al. (2012) conclude that an increase in temperature can be associated with a decrease in the height of the "bee" structures.

Dourado et al. (2012), measured mechanical properties of the asphalt bitumen by means of AFM. Significant differences were observed in the elasticity of the bitumen in the "bee" structure and the continuous phase. Indentations were also performed on the "bee" structures. It was found that the elastic recovery is dependent on the colloidal structure of the "bee".

Nazzal and Qtaish (2012) observed that the "bee" structures are present in both neat and polymer modified bitumen. However, the use of a Sasobit additive (crystalline, long chain aliphatic polymethylene hydrocarbon) reduced the dimensions of the structure. Additionally, the Sasobit increased the relative stiffness of the dispersed domains that contained the aforementioned structure. This in turn correlated to the higher shear modulus observed on a DSR.

Furthermore Jäger et al. (2004), looked into the chemical composition of the "bee" structures. The researchers found that the "bee" structures are present when asphaltenes are precipated by the addition of n-heptane. However, no structures such as the previous or hard surfaces are present in the maltene phase. This would be consistent with the theory that the "bee" structures are related to the wax content present in the asphaltenes.

4.0 Objectives

The study focuses on analyzing the morphology of the asphalt bitumen based on AFM topography and phase imaging. Additionally, an effort is also made towards identifying the source of the "bee" structures: asphaltenes, presence of polymers, product of oxidation process, or crystallization of paraffinic waxes in the bitumen.

Towards this goal, a chromatographic separation and further analysis of the different components of the asphalt bitumen is also performed with the intention of

determining which components, or combination of components, results in different structures and phases.

5.0 Materials Used in the Study

The bitumen that was used is this study corresponds to a viscosity grade AC-30 (PG64-22) obtained from RECOPE (Costa Rican Petroleum Refinery). This bitumen represents the most common bitumen used in Costa Rican roads. A chromatography analysis made using the chromatography column (ASTM 4124) showed that the SARA fractions of the neat bitumen are distributed as follows: saturated (7.3±0.3)%, aromatics (43.5±0.7%), resins (33.5±0.8)% and, asphaltenes (16.6±0.5)% (Stability index = 0.3).

To evaluate the effect of a polymer modifier on the neat bitumen morphology, a SBS modified bitumen was also prepared (neat bitumen + 2.5% w/w SBS).

6.0 AFM Analysis

The analysis has been performed with a Witec Alpha 300 AFM, using AC mode. Measurements were performed on the neat asphalt bitumen and on the different SARA components of the material. Additionally, the 1:1 and 1:1:1 combinations of the different components were also analyzed to observe if the different phases present in the bitumen are the result of combinations of different components. Furthermore, asphalt bitumen enriched with the various SARA separated components was also evaluated.

The analyzed samples were prepared using solvent-cast films of the asphalt bitumen and its different components. The solvent that was used corresponds to trichloroethylene (TCE) and was allowed to evaporate at room temperature. This is clarified since Masson et al. (2006), Pauli et al. (2009), and other researchers have pointed out that differences can be observed when casting the asphalt films by means of heat or solvent.

The images that were obtained from the AFM provide information on the topography, but using phase detection, also allow for the identification of the different phases present. Figure 1 shows the AFM measurements of the neat bitumen, which based on previous research corresponds to a multi-phase type bitumen. From the figure, the sal-phase, para-phase, per-phase, and catana-phase can be identified. The catana-phase corresponds to the "bee" structures and the per-phase corresponds to the area surrounding the catana-phase. The para-phase is the matrix or continuous phase and the sal-phase are smaller segregated particles in the para-phase.

(a)

(b)
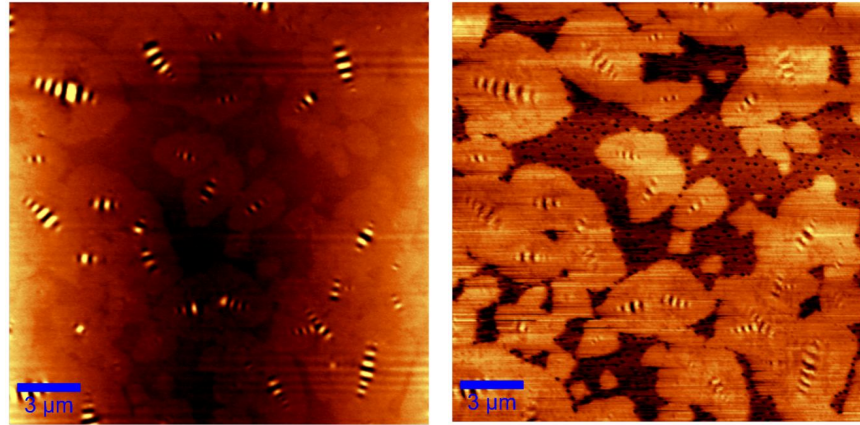
Figure 1. *(a) Topographic and (b) Phase image of neat asphalt binder (20 μm x 20 μm)*

(a)

(b)
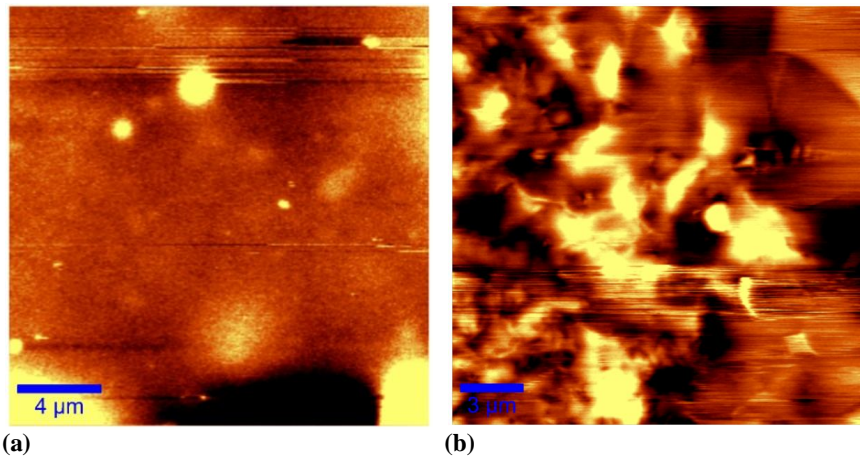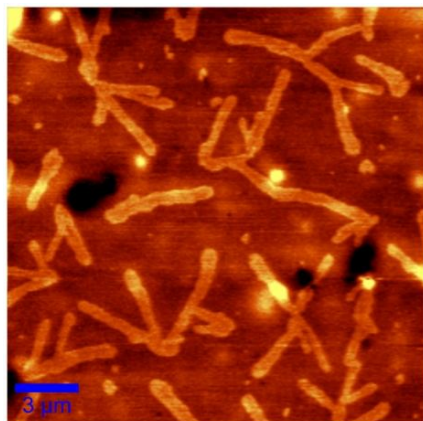
(c)

Figure 2. *Topographic images for (a) asphaltenes, (b) aromatics, and (c) resins (20 μm x 20 μm)*

Figure 2 shows the AFM topographic images of the different SARA fractions or bitumen components. The phase images associated to Figure 2 also show the same structure and phase patterns. The saturates could not be measured because of their oily behavior, which resulted in interference with the cantilever tip. The paraffin in the asphalt bitumen would be present in the saturates.

The obtained images can provide information on the roughness/topography of the different components. However, more valuable is provided by the analysis of the phases which allows for determining the possible source of the "bee" structures as shown in Figure 3. The images indicate that the "bee" structure is not associated to the asphaltenes since the phase does not exhibit them. However, a feasible precursor of this structure type is present in the aromatics (naphthenic aromatics). Furthermore, a structure (filament-type) that cannot be observed on the asphalt bitumen directly is present on the resins (polar aromatics). Both the asphaltenes and the resins also show indications of the sal-phase previously described by Masson et al. (2006). This can be an indicator of the affinity between the two components.

Figure 3 corresponds to 100x optical images of the same SARA components. The same structures observed on AFM can be captured at the optical level. Additionally, optical imaging allowed for capturing of the saturate component. It can be observed from the image that the saturates do not appear to exhibit the per-phase or the catana-phase, or the "bee" structures. This can serve as an indication that the aforementioned phases do not necessarily correlate to the crystallization of paraffin waxes, since this waxes are primarily present in the saturates.
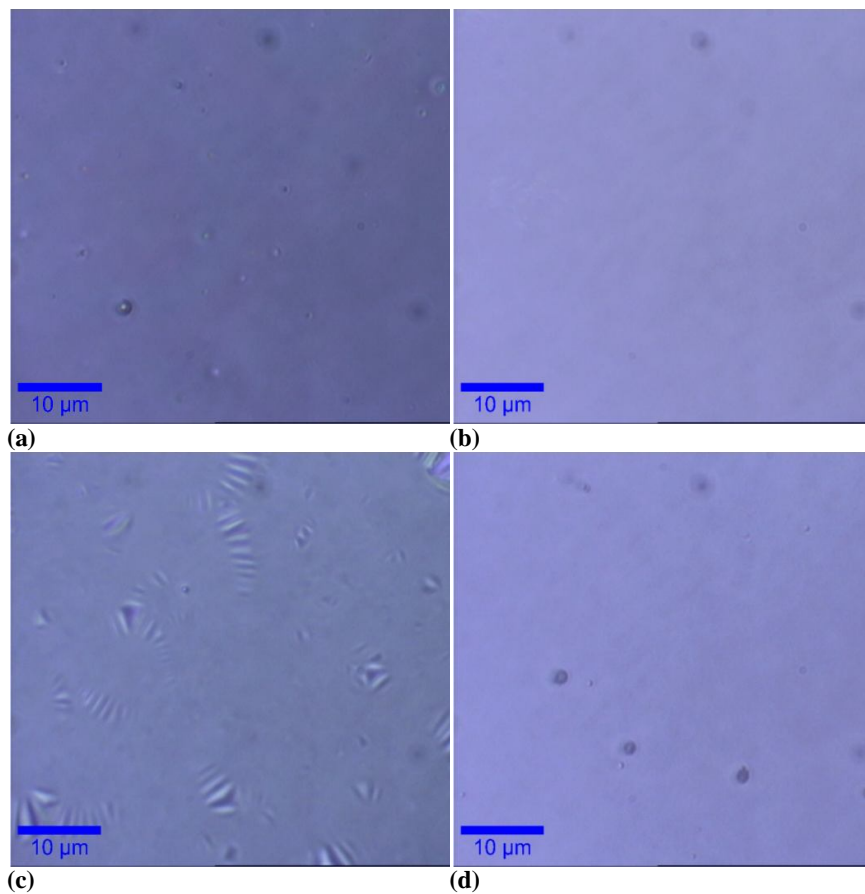
Figure 3. *100x optical images for (a) asphaltenes, (b) saturates, (c) aromatics, and (d) resins (60 μm x 60 μm)*

To determine the phases that result of the combination between the different components of the asphalt bitumen, 1:1 combinations were generated and observed under AFM. Figure 4 shows the combination of asphaltenes with the remaining components. Because of the high polarity of asphaltenes, they exhibit a high tendency to associate with the other components.

(a)

(b)

(c)

(d)

(e)
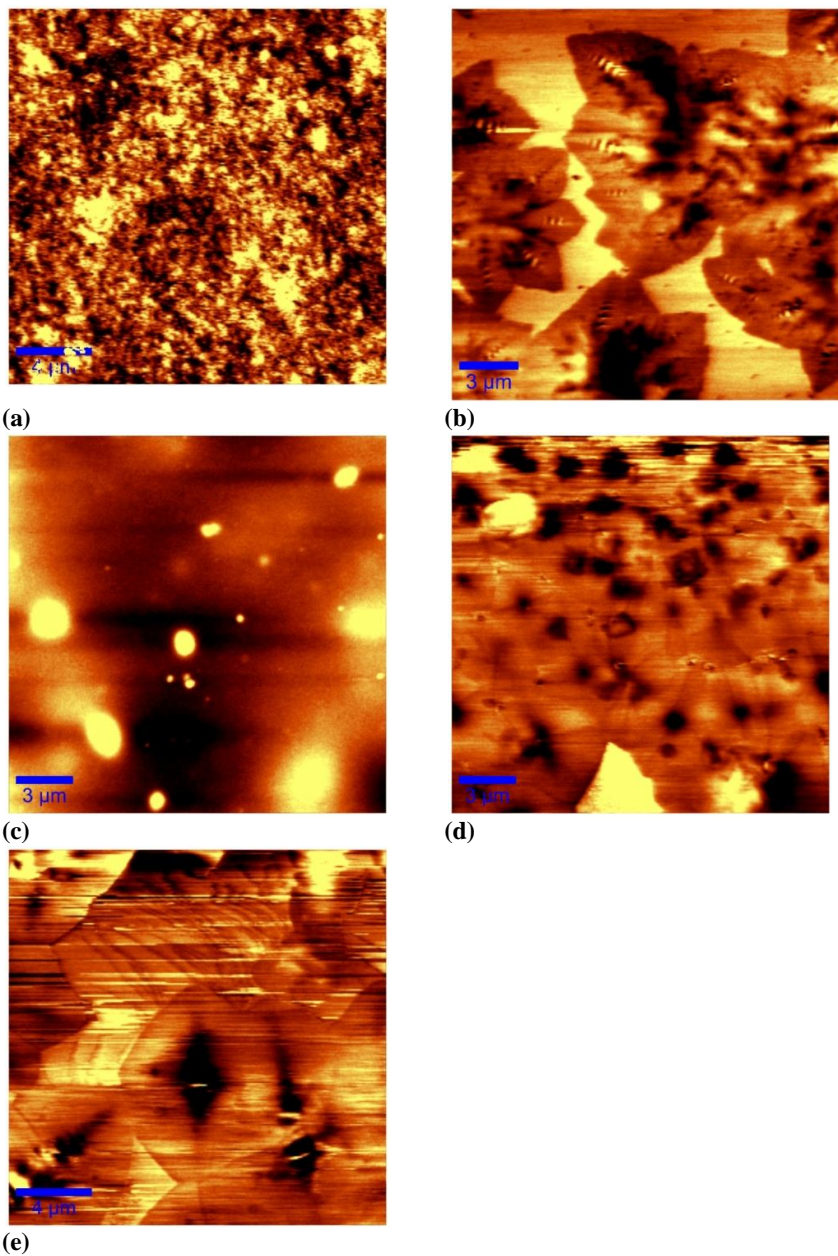
Figure 4. *Topographic images for 1:1 combination of asphaltenes with (a) saturates, (b) aromatics, (c) resins, and aromatics with (d) saturates and (e) resins (20 μm x 20 μm)*

The figure shows clear evidence that the "bee" structures break up into smaller components when the aromatics (containing the "bee" structures) combine with the asphaltenes. This results into a conglomerate of catana-phase ("bee" structure) within a single per-phase. Additionally, as was expected, the compatibility between the asphaltenes and the resins is high and the resulting structure is similar to that of the individual components. Note, however, that the filament-type structure that was identified in the resins does no longer appear visible. Up to this point, evidence indicates that the aromatics is the component responsible for the existence of the "bee" structure or catana-phase.

Figure 4 also presents the remaining combinations that could be measured with the AFM. The 1:1 combination between saturates and resins could not be captured properly. The combination between saturates and aromatics indicates that there is a dominance between the phases associated to the saturates and waxes, to that of the aromatics. In the case of the combination between the aromatics (naphthenic aromatics) and resins (polar aromatics), because of the polarity differences between the components, it appears that the structures tend to group together but do not combine. However, the presence of the filament-type phase could not be observed.

Finally, combinations of three out of four SARA components were prepared in 1:1:1 ratios. The AFM results are shown on Figure 5. It can be observed that the combinations result in the four main phases associated with a multi-phase type bitumen. However, note that the size of the per- and catana-phase differ considerably. The "bee" structures are associated with the aromatic component of the asphalt bitumen. Additionally, it is evident that the presence of asphaltenes results in a reduction of the size of the aforementioned phases. In contrast, the presence of resins results in an increase in the size of these phases.
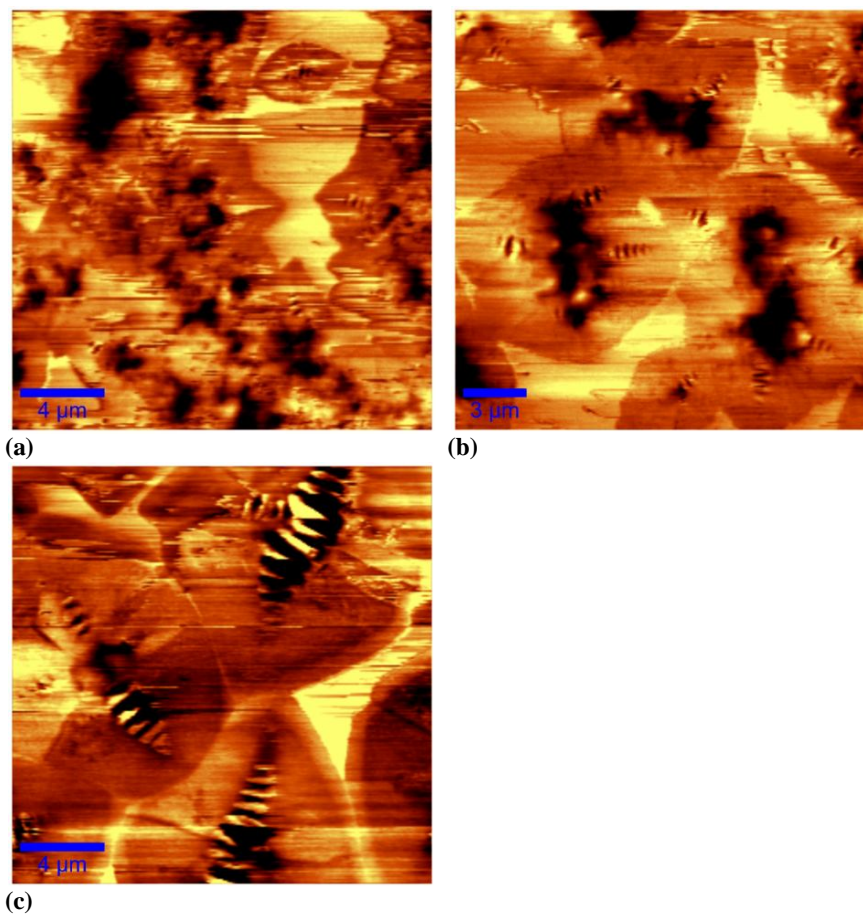
Figure 5. *Topographic images for 1:1:1 combinations of (a) asphaltenes, saturates, and aromatics, (b) asphaltenes, aromatics, and resins, and (c) saturates, aromatics, and resins (20 μm x 20 μm)*

To complement the previous analysis, and to observe the effect of the different SARA components on the asphalt bitumen morphologhy, enriched asphalt bitumen was produced by incorporating an additional 50% of each of the SARA fractions (saturates, resins, and aromatics) to the asphalt bittumen matrix, as measured by column chromatography. In the case of the asphaltenes, the dosified content was approximately 15% due to difficulty associated with increasing the asphaltene content. Only one of the four different components was included at any given time in order to observe the effect of the component. The topographic and phase AFM

images are shown on Figures 6 and 7. As opposed to the previous analysis, the asphalt bitumen enriched with saturates was be measured.

(a)

(b)

(c)

(d)
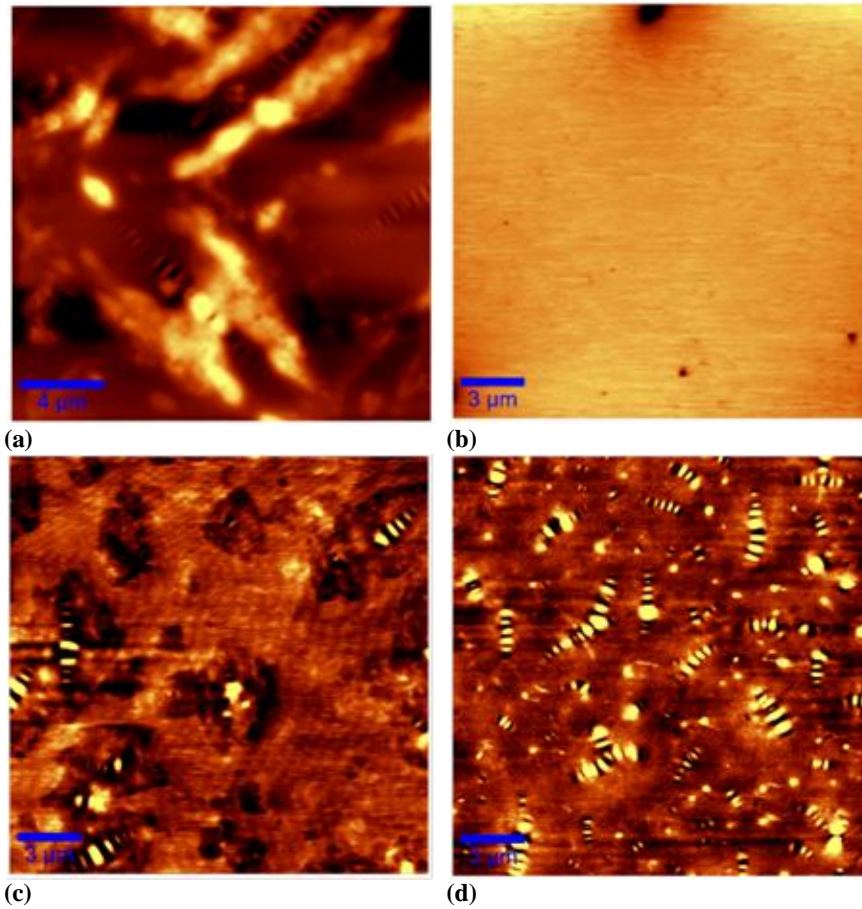
Figure 6. *Topographic images for asphalt binder enriched with (a) asphaltenes, (b) saturates, (c) aromatics, and (d) resins (20 μm x 20 μm)*
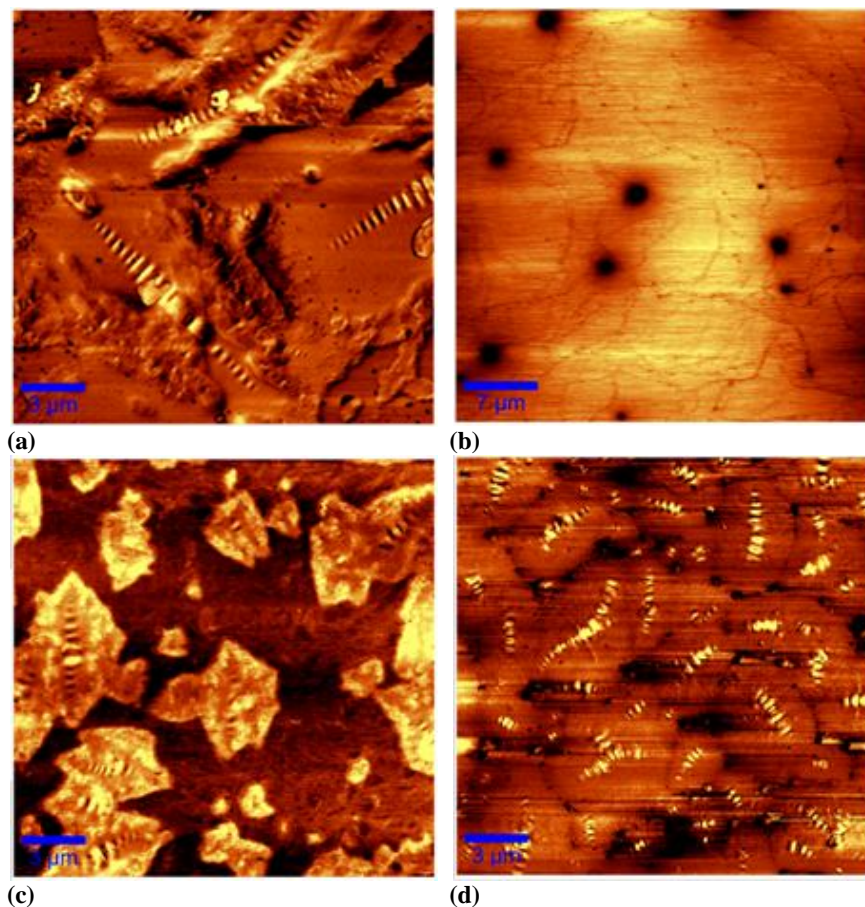
Figure 6. *Phase images for asphalt binder enriched with (a) asphaltenes, (b) saturates, (c) aromatics, and (d) resins (20 μm x 20 μm)*

The images indicate that the enriched asphalt bitumen also exhibits the 4 phases that were identified on the neat bitumen. However, the overall shape of the different phases is affected by the enrichment with the different components. In the case of asphaltenes, the catana-phase increases in length. However, the difference between the per-phase and para-phase is no longer evident. Similarly, the sal-phase appears to have combined with the catana-phase in several of the "bee" structures.

In the case of asphalt bitumen enriched with aromatics (which were originally identified to contain the per- and catana-phase), the intensity of the both the per-phase and catana-phase increases. However, when the asphalt binder is enriched with resins, the overall size of the "bee" structures (catana-phase) remains similar to

the neat bitumen; however, the area of the per-phase does increase, reducing the area that was originally ocuppied by the para-phase. Finally, the bitumen enriched with saturates corresponds to a continuous medium with variable topography changes. Also note that only in the case of the saturate enriched asphalt bitumen, the per-phase, catana-phase, and the sol-phase appear to be absent in both the topographic and phase images.

7.0 FTIR Analysis of Asphalt Bitumen Components

Figure 8 shows the FTIR spectrums for the 4 different SARA components of the analyzed asphalt bitumen. The technique was used to characterize the molecular structure of the materials (Kuptsv, 1994). Additionally, the figure also shows the neat asphalt binder for comparison purposes.
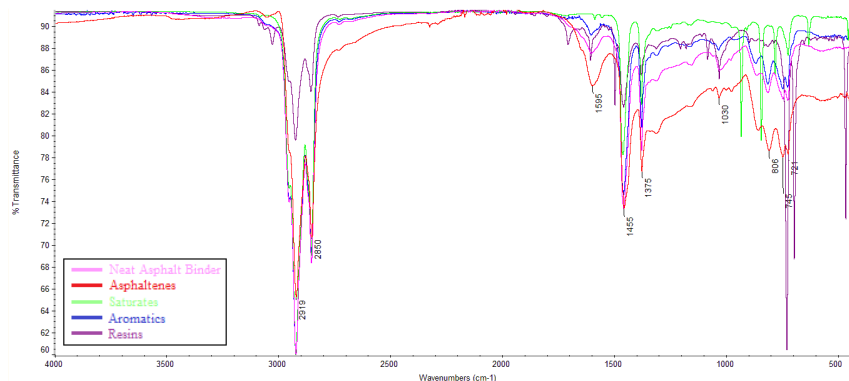
Figure 8. *FTIR spectra for asphalt bitumen and bitumen components*

The characteristic bands for the different phases were summarized on Table 1. The differences in the singular components of the asphalt bitumen are highlighted with respect to the neat asphalt bitumen. The asphaltenes correspond to a large fraction of complex polar aromatic compounds that are highly insoluble in paraffinic solvents such as n-heptane and are solid at room temperature. Because of the type of interactions, they present bands typical of the asphalt bitumen. Additionally, because of the separation process, the sample may be contaminated with other phases due to the string interactions with other components.

The saturates are a non polar viscous fraction, composed mainly of long lineal chains with aliphatic ramifications of different magnitudes. The aromatics are mainly aromatic rings, linked by linear chains with or without ramifications with methyl. Consequently this fraction can serve as solvent for asphaltenes. Finally, the resins are formed of mainly highly polar compounds of adhesive nature, with a solid to semi-solid consistency. It is believed that the resins stabilize the asphaltenes by peptization and govern the colloidal nature of the asphalt binder.

**Table 1.** *Spectrum Bands Associated with SARA Fractions*

Wavelength (cm⁻¹)	Neat Asphalt Binder	Asphaltenes	Saturates	Aromatics	Resins
3030	-	-	-	-	**Low intensity band of C=CH₂ (Ar) (***Aromatic alkenes***)**
2851- 2920	High intensity band of CH₂ and CH₃ groups (*Saturated hydrocarbons*)	High intensity band of CH₂ and CH₃ groups (*Saturated hydrocarbons*)	High intensity band of CH₂ and CH₃ groups (*Saturated hydrocarbons*)	High intensity band of CH₂ and CH₃ groups (*Saturated hydrocarbons*)	**Medium intensity band of CH₂ and CH₃ groups (***Saturated hydrocarbons***) lower intensity**
1705	-	-	-	-	**Low intensity band of C=CH₂ (Ar) (***External alkenes***)**
1600	Low intensity band of C=C (Ar) (*Aromatic hydrocarbons*)	Medium intensity band of C=C (Ar) (*Aromatic hydrocarbons*) **intensified**	-	Low intensity band of C=C (Ar) (*Aromatic hydrocarbons*)	Low intensity band of C=C (Ar) (*Aromatic hydrocarbons*)
1500	Medium intensity band of C=C (Ar) (*Aromatic hydrocarbons*)	Medium intensity band of C=C (Ar) (*Aromatic hydrocarbons*)	-	Medium intensity band of C=C (Ar) (*Aromatic hydrocarbons*) **Lower intensity - possibly combined with 1460 cm⁻¹ band**	Medium intensity band of C=C (Ar) (*Aromatic hydrocarbons*)
1450	Medium intensity band of CH₂ and CH₃ groups (*Saturated hydrocarbons*)	Medium intensity band of CH₂ and CH₃ groups (*Saturated hydrocarbons*)	Medium intensity band of CH₂ and CH₃ groups (*Saturated hydrocarbons*)	Medium intensity band of CH₂ and CH₃ groups (*Saturated hydrocarbons*)	Medium intensity band of CH₂ and CH₃ groups (*Saturated hydrocarbons*)
1340	Medium intensity band of C-N (*Aromatic Amines*)	Medium intensity band of C-N (*Aromatic Amines*)	Medium intensity band of C-N (*Aromatic Amines*) and **-CH₃ groups** (***External Methyl - 2 singlets***)	Medium intensity band of C-N (*Aromatic Amines*)	Medium intensity band **possibly** of C-N (*Aromatic Amines*)
1170	Low intensity band of R-O-Ar (*Alkyl aryl ethers*)	Low intensity band of R-O-Ar (*Alkyl aryl ethers*)	-	-	Low intensity band of R-O-Ar (*Alkyl aryl ethers*) **Lower intensity**
1030	Low intensity band of R-O-Ar (*Alkyl aryl ethers*)	Low intensity band of R-O-Ar (*Alkyl aryl ethers*)	-	Low intensity band of R-O-Ar (*Alkyl aryl ethers*) **Lower intensity**	Low intensity band of R-O-Ar (*Alkyl aryl ethers*) **Lower intensity**
931	-	-	**Medium intensity band of -CH₃ groups (***Saturated hydrocarbons***)**	-	**Very low intensity band of -CH₃ groups (***Saturated hydrocarbons***)**
841	-	-	**Medium intensity band of -CH₃ groups (***Saturated hydrocarbons***)**	-	**Very low intensity band of -CH₃ groups (***Saturated hydrocarbons***)**
780	-	-	**Medium intensity band of -CH₂ -groups (***Saturated compounds of long linear chain***)**	-	**Very low intensity band of -CH₂ -groups (***Saturated compounds of long linear chain***)**
750	Low intensity band of C-H meta (*Aromatic compounds*)	Low intensity band of C-H meta (*Aromatic compounds*) **lower intensity**	-	Low intensity band of C-H meta (*Aromatic compounds*)	-
730	-	-	-	-	**Very high intensity band of C-H meta (***Aromatic compounds***)**
720	Low intensity band of C-H para (*Aromatic compounds*)	Low intensity band of C-H para (*Aromatic compounds*) **lower intensity**	**Medium intensity band of -CH₂ -groups (***Saturated compounds of long linear chain***)**	Low intensity band of C-H para (*Aromatic compounds*) and **Medium intensity band of -CH₂ - groups (***Saturated compounds of long linear chain***)**	-
680	-	-	**Low intensity unidentified band**	-	**Very high intensity band of C-H para (***Aromatic compounds***)**
460	-	-	-	-	**High intensity band of Ar-C-H or Ar-S-H (***Aromatic compounds***)**

(*) The comments in **bold** are made with respect to the neat asphalt binder.

8.0 Effect of Polymers and Temperature on Asphalt Bitumen Morphology

Verification on the effect of the incorporation polymers, and the temperature effects, on the morphology of asphalt binder was performed to evaluate the hypothesis that the phases present in the asphalt binder are associated with these external factors. Figure 9 shows the topographic images for the analyzed conditions.

(a)   **(b)**
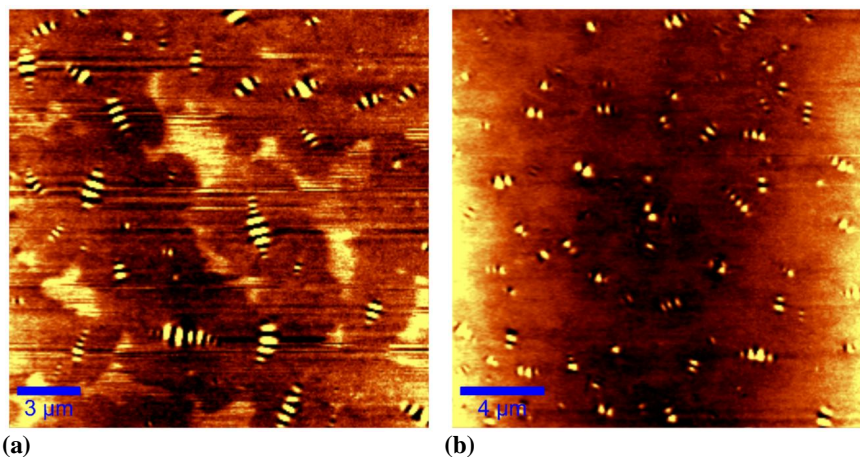
Figure 9. *Topographic images of (a) polymer modified and (b) temperature aged asphalt bitumen (20 μm x 20 μm)*

In the case of the polymer modified asphalt bitumen, 2.5% w/w SBS polymer was added to the neat bitumen at a modification temperature of 185°C during a period of 3.5 hours. The figure indicates an important reduction in the size of the para-phase and an increase in the size of the per-phase. In appearance, the resulting morphology is similar to the one observed when enrichment with resins was performed on the neat asphalt bitumen.

To isolate the impact of possible aging during the modification process, the effect on the morphology of the asphalt bitumen was also evaluated when the neat asphalt bitumen is subjected to 30 minutes of aging at 185°C. The higher temperatures resulted in a reduction of the per-phase and catana-phase ("bee" structure). In general, it is expected that aging result in morphological changes that will be associated to changes in micro-mechanical behavior. However, the different phases associated with the neat asphalt bitumen are all still present.

9.0 Summary of Findings and Conclusions

The obtained topographic and phase AFM images allow for determining of the different phases that are present within the different components of the asphalt bitumen. Observation of the source of the "bee" structures was emphasized. The measured results seem to corroborate that the source of the "bee" structures is not related to the asphaltenes. Furthermore, the hypothesis that the "bee" structures correspond to oxidation products, modification of asphalt bitumen with polymers, or crystallization of paraffinic waxes within the asphalt bitumen seems unlikely. Nonetheless, there is clear evidence that temperature aging of the asphalt bitumen has an effect on the morphology of the material, and as such, on the different structures that are present within the different SARA components. Similarly, the addition of a polymer modifier resulted in changes to the different phases associated with the asphalt bitumen. This is expected since a foreign compound is being incorporated into the asphalt bitumen matrix.

The phase images that were obtained of the different components indicate that the "bee" structures are correlated with the aromatics (naphthenic aromatics). Both the 20 x 20 μm and the 100X optical image corroborate the presence of "bee" structures in the aromatic component of the asphalt bitumen. Additionally, optical microscopy could not detect the presence of per-phase and catana-phase ("bee" structures) on the saturates, which is the component of the asphalt bitumen that contains paraffinic waxes. In general, even though the source of the "bee" structures appears to be directly related to the aromatics (naphthenic aromatics), the size, shape, and topography of the structure is associated to the combination of different components associated with the asphalt bitumen. This was verified by enrichment of the asphalt bitumen with 50% of each of the SARA fractions (saturates, resins, and aromatics), and analyzing each combination at a time.

Finally, even thought the source of the "bee" structures might be related to the aromatics, the focus of further analysis should be related to the phase changes associated with this structure type. Consequently, additional research is currently being performed to quantify the micro-mechanical behavior associated with the different SARA components and phases present within each component and combinations thereof. Same type of analysis is being performed when the asphalt bitumen is perturbed with the addition of an additive, or when it is subjected to controlled changes in temperature, humidity, and oxygen.

8. Bibliography

Allen, R.G. structural characterization of micromechanical Properties in asphalt using atomic force microscopy. M.Sc. Thesis. College Station, TX. 2010.

Allen, R., Little, D., Bhasin, A. Structural Characterization of Micromechanical Properties in Asphalt Using Atomic Force Microscopy. J. Mater. Civ. Eng., Vol. 24, Issue 10, pp. 1317–1327. 2012.

Asphalt Institute. The asphalt handbook. Manual Series No. 4 (MS-4), The Asphalt Institute, Lexington, KY,. 1989.

Beaulieu, L.Y., Godin, M., Laroche, O., Tabard-Cossa, V., Grütter, P. Calibrating laser beam deflection systems for use in atomic force microscopes and cantilever sensors. Applied Physics Letters, Vol. 88, Issue 8, pp. 083108-1–083108-1. 2006.

Burnham, N.A., Colton, R.J. Measuring the nanomechanical properties and surface forces of materials using an atomic force microscope. Journal of Vacuum Science & Technology A, Vol. 7, Issue 4, pp. 2906-2913. 1989.

Dourado, E.R., Simao, R.A., Leite, L.F.M. Mechanical properties of asphalt binders evaluated by atomic force microscopy. Journal ofMicroscopy, Vol. 245, Issue 2, pp. 119–128. 2012.

Jäger, A., Lackner, R., Eisenmenger-Sittner, C., Blab, R. Identification of four material phases in bitumen by atomic force microscopy. Journal of Road Materials and Pavement Design, Vol. 5, Supl. 1, pp. 9-24. 2004.

Jäger, A., Lackner, R., Eisenmenger-Sittner, C., Blab, R. Identification of Microstructural Components of Bitumen by Means of Atomic Force Microscopy (AFM). Proc. Appl. Math. Mech., Vol. 4, Issue 1, pp. 400–401. 2004.

Krishnan, J., Rajagopal, K.R. On the mechanical behavior of asphalt, Mechanics of Materials, Vol. 37, Issue 11, 2005, pp. 1085-1100.

Kuptsov, A.H. Applications of Fourier Transform Raman Spectroscopy in Forensic Science. Journal of Forensic Sciences, JFSCA, Vol. 39, No. 2, pp. 305-318. 1994.

Loeber, L., Sutton, O., Morel, J., Valleton, J.M., Muller, G. New direct observations of asphalts and asphalt binders by scanning electron microscopy and atomic force microscopy. Journal of Microscopy, Vol. 182, Issue 1, pp. 32–39. 1996.

Macoski, C.W. Rheology: principles, measurements, and applications. Wiley VCH. 1993.

Masson, J.F., Leblond, V., and Margeson, J. Bitumen morphologies by phase-detection atomic force microscopy, Journal of Microscopy., Vol. 221, Issue 1, pp. 17–29. 2006.

Masson, J.F., Leblond, V., Margeson, J. Low-temperature Bitumen Stiffness and Viscous Paraffinic Nano- and Micro-Domains by Cryogenic AFM and PDM. Journal of Microscopy, Vol. 227, Issue 3, pp. 191-202. 2007.

McCarron, B., Yu, X., Tao, M., Burnham, N. The Investigation of 'Bee-Structures' in Asphalt Binders. Qualifying Project. Worcester, MA. 2012.

Meyer, G., Amer, N. Novel optical approach to atomic force microscopy. Applied Physics Letters, Vol. 53, Issue 12, pp. 1045-1047. 1988

Moraes, M.B.d., Pereira, R.B., Simao, R.A., Leite, L.F.M. High temperature AFM study of CAP 30/45 pen grade bitumen. Journal of Microscopy, Vol. 239, Issue 1, pp. 46-53. 2010.

Nazzal, M.D., Qtaish, L.A. The Use of Atomic Force Microscopy to Evaluate Warm Mix Asphalt. Report FHWA/OH-2012/19. Athens, OH. 2012.

Pauli, A.T., Grimes, R.W., Beemer, A.G., Miller, J.J., Beiswenger, J.D., Branthaver, J.F. Studies if the Physico-Chemical Nature of the SHRP Asphalts: PART-I & II. Proceedings of the international workshop on chemo-mechanics of bituminous materials, pp. 25-30, 49-53. Delft, The Netherlands, 2009.

Roa, J. J., Oncins, G., Díaz, J., Sanz, F., and Segarra, M. Calculation of Young's Modulus Value by Means of AFM. Recent Patents on Nanotechnology, Vol. 5, pp. 27-36. 2011.

West, R.C., Watson, D.E., Turner, P.A., Casola, J.R. Mixing and Compaction Temperatures of Asphalt Binders in Hot-Mix Asphalt. NCHRP REPORT 648. Washington, D.C., 2010.